AJChE 2006, Vol. 6, No. 1, 8–21

Dynamic Cycling State of Nonadiabatic Catalytic Combustion of Propylene Using Flow Reversal

Suryo Purwono
Chemical Engineering Department
Gadjah Mada University
Jl. Grafika No. 2, Yogyakarta, INDONESIA
Email: spurwono@chemeng.ugm.ac.id

An experimental study of nonadiabatic fixed-bed reactor for controlling propylene gas was made under flow reversal operation. Temperature measurements were made within the catalyst and packing beds. The influence of the operating parameters on the shape of temperature profiles, conversion, and heat removal were studied. The experiments showed that the maximum measured reactor temperature and heat removal were rather insensitive to changes in cycle duration and sensitive to feed flow rate and reactant concentration. The simulation results for the variation of concentration, flow rate, and cycle time showed the experimentally observed behavior Further simulations showed that runaway can occur when concentration was high.

Keywords: Catalytic combustion, flow reversal, nonadiabatic fixed bed reactor, propylene, *and* runaway.

INTRODUCTION

Flow reversal technology is a relatively new technique for handling exothermic reaction in fixed bed reactors. The idea of periodic reversal of the flow direction comes from Russian researchers (Boreskov et al. 1977). They used simulation to explore the concept based on a one-dimensional unsteady state mathematical model.

After the pioneering investigation of Boreskov et al. (1977), many researchers have worked experimentally and analytically on flow reversal (Boreskov et al. 1982, Eigenberger and Nieken 1988, Gawdzik and Rakowski 1989, Matros 1989 and 1990, Blank et al. 1990, Bathia 1991, Gupta and Bathia 1991, and Rehacek et al. 1992). There have been also studies on industrial scale plants (Matros 1989, 1990).

Matros (1989, 1990) studied the possibility of using flow reversal technology, analytically and experimentally, for the purification of gas–air mixture containing small amounts of carbon monoxide, methane, or other combustible substances which formed during the various processes.

Several researchers have worked using flow reversal technology in processes other than SO_2 oxidation and purification of combustible gases. Blank et al. (1990) proposed this technique for the production of synthesis gas, carbon monoxide, and hydrogen from catalytic partial oxidation of natural gas with air. Froment (1990) reported on the operation of a reversal flow reactor for low-pressure methanol synthesis.

In 1992, Haynes et al. proposed the application of a reverse flow reactor to endothermic reactions for the dehydrogenation of ethyl benzene.

Despite the studies mentioned in Boreskov et al. 1977 and 1983 and Matros 1989 and 1990), however, there was no published work on the handling of runaway when feed concentration suddenly increases. So far the flow reversal process has been carried out using two adiabatic reactors connected to each other with a heat exchanger placed between them. In this kind of process, however, it is difficult to control runaway. Therefore, the present reasercher proposed to improve the technique of handling low gas concentrations by integrating a fixed bed reactor with a heat exchanger for removing heat directly from the system.

Matros (1989) and Boreskov et al. (1986) have successfully predicted the thermal behavior of the unsteady-state process in the above designed adiabatic reactors. In this model, the temperature distribution in the radial position had been omitted since adiabaticity is assumed. However, in the nonadiabatic operation discussed here the radial gradients must now be included.

EXPERIMENTAL AND PROCEDURE

Equipment and procedure

Figure 1 shows the diagram of the experimental set-up. All gases flowing to the reactor were dried over filters containing 4A molecular sieves and anhydrous calcium sulphate to reduce traces of impurities. Brooks 5850 flow transducer-controllers regulated the feed mass flow rate into both the reactor and the heat exchanger when air from the system was used as coolant. They permitted only uni-directional flow and, therefore, acted as check valves. This feature ensured that during flow reversal, for instance, there would be no backflow immediately after switching.

The three ways Tomco 95 solenoid valves controlled by a ChronTrol CD 03 timer were used for flow reversal operation when particular feed mixtures were fed into the system at preset times. The system operating pressure was measured using Matheson pressure gauges. All the thermocouples in the system were connected to an Instrulab 2000 data logger. The effluent concentrations of the carbon dioxide formed from the reaction were measured using an on-line IR spectrophotometer IR-702 D dual analyser supplied by Infrared Industries, Inc. This unit was capable of continuously monitoring CO_2 concentrations in the product stream simultaneously.

The reactor was 15-cm long and 1-cm ID stainless steel tubing with a cooler surrounding it and connected to a 30-cm length of packing which had 1.6-cm ID as a preheater at each end. To prevent catalyst packing ball movement, stainless steel screens were installed at the inlet and outlet of the reactor.

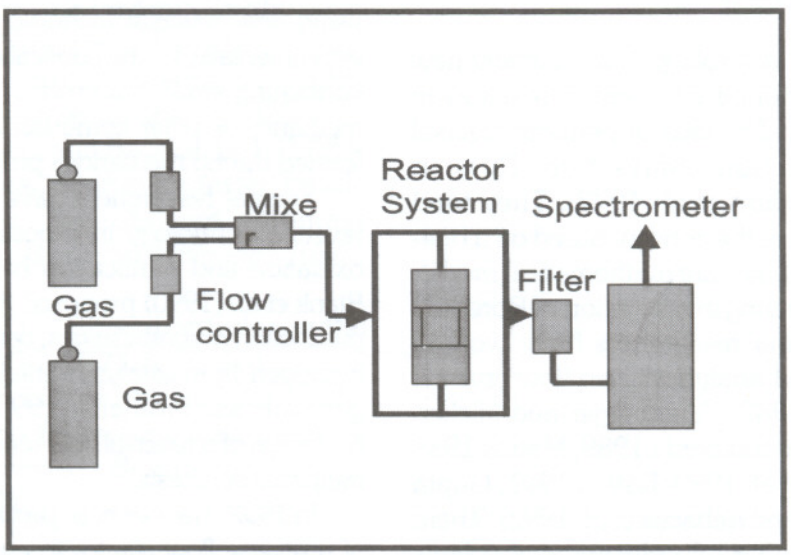

Figure 1. Schematic of the Experimental Set-up

Nine 1.6-mm OD chromel-alumel thermocouples were placed in each packing zone and seven 0.508-mm OD chromel-alumel thermocouples were inserted in the reaction zone to monitor the temperature distribution as reaction proceeded. To make sure that the thermocouples only read the gas temperature, they were jacketed using ceramic thermocouple protection tubes.

Four 1.6-mm OD chromel-alumel thermocouples were placed in the cooling system. Two of them were used to measure the inlet and outlet coolant temperatures. The other two were used to measure the reactor wall temperatures. These four thermocouples were not jacketed.

For each run, the reactor was first preheated to slightly above desired reaction temperature using a heating tape wrapped along the gas tubing. To make sure that the temperature in the system was uniform, preheated hot air was flowed into the system. When a constant temperature was reached, the heating tape was turned off and the cold reaction mixture was introduced into the system. As this mixture passed through the hot packing, it absorbed heat. As the packing cooled, the mixture was heated to the reaction temperature and reacted over the catalyst.

The exothermicity thus released raised the temperature of the catalyst bed. The heat carried by the hot gas to the second packing zone formed a slowly migrating front moving towards the outlet in that zone. After some time, the region in the inlet of the reactor would cool as heat transferred from the packing *zone* to the feed gas. Meanwhile, the outlet region was heated by the exothermic reaction. The direction of the gas mixture would be reversed, and the reaction wave would start to creep to in the opposite direction in the two packing zones. After some time the whole cycle would be repeated.

This cyclical process created a hot region in the catalyst bed which could be used as a heater or boiler. The temperature profiles along the reactor were monitored and recorded in a data logger during the process. The monitoring and recording of temperatures were started when the cold reactant was first introduced to the reactor. The carbon monoxide and carbon dioxide concentrations of the gas leaving the system were monitored continuously with an on-line analyzer. The monitoring of the concentration was also started when the cold reactant was first introduced.

Catalyst used in the process

Granulars of the catalyst, platinum and palladium on zeolite, developed in the laboratory were used in the process (Purwono et al. 1997). The metal on zeolite catalysts contained 2 to 4 % metal, the metal being deposited as a shell surrounding the catalyst particle supplied as 3.18 x 10^{-3} m time 3.18 x 10^{-3} m tablet. The characteristics of the catalysts are shown in Table I. The catalyst was found to have very stable activity. Except for a slight initial decay, the activity remained constant with prolonged use.

Table 1. Catalyst Properties

Properties	Dimensions
Surface area	2.01 x 10^5 m^2/kg
Bulk density	1.8 x 10^3 kg/m^3
Total pore volume	2.4 x 10^{-4} m^3/kg

In this research, 99% purity of propylene was used in the feedstock. Propylene, which was chosen because its oxidation could be initiated at relatively low temperatures (» 200°C), is an important industrial waste gas. Catalytic oxidation is often used to render this gas inert by converting it to CO_2.

MATHEMATICAL MODEL

A model capable of describing a nonadiabatic fixed bed flow reversal reactor must have parameters to describe the heat fluxes from gas dispersion, interphase transfer, and solid phase conduction.

Actually, three types of transport processes are involved in the operation of a heterogeneous system in a fixed bed reactor (Froment and Bischoff 1989): Interparticle transport through the voids between the catalyst pellets, intraparticle transport within the catalyst pellet,

and interphase transport between the mainstream of the fluid and the surface of the catalyst pellet. However, to keep the model reasonably simple, assumptions are needed.

The energy balance for the gas and solid phases involves four assumptions: axial gas velocity is independent of radial position, voids in the packing are uniformly distributed, negligible radiation occurs, and no radial temperature gradient occurs inside a particle. With the above assumptions, a set of mathematical models had been developed as shown below using cylindrical coordinates.

The energy and mass balances for the gas and solid phases in the packing and catalyst zones are as follows:

Energy balance

Packing zones

Solid phase

$$\frac{\partial T_s}{\partial t} = \frac{k_{esax}}{\rho_s Cp_s}\frac{\partial^2 T_s}{\partial Z^2} + \frac{k_{esr}}{\rho_g Cp_s}\left(\frac{1}{r}\frac{\partial}{\partial r}\left(r\frac{\partial T_s}{\partial r}\right)\right) - \frac{h a_v}{\rho_s Cp_s(1-\varepsilon)}(T_s - T_g) \quad (1)$$

Gas phase

$$\frac{\partial T_g}{\partial t} = \frac{k_{egax}}{\rho_g Cp_g}\frac{\partial^2 T_g}{\partial Z^2} + \frac{k_{egr}}{\rho_g Cp_g}\left(\frac{1}{r}\frac{\partial}{\partial r}\left(r\frac{\partial T_g}{\partial r}\right)\right) - \frac{h a_v}{\rho_g Cp_g \varepsilon}(T_s - T_g) - V\frac{\partial T_g}{\partial Z} \quad (2)$$

Catalyst zone

Solid phase

$$\frac{\partial T_s}{\partial t} = \frac{k_{esax}}{\rho_s Cp_s}\frac{\partial^2 T_s}{\partial Z^2} + \frac{k_{esr}}{\rho_g Cp_s}\left(\frac{1}{r}\frac{\partial}{\partial r}\left(r\frac{\partial T_s}{\partial r}\right)\right) - \frac{h a_v}{\rho_s Cp_s(1-\varepsilon)}(T_s - T_g) + \frac{(-\Delta H)(-r_c)}{Cp_s} \quad (3)$$

Gas phase

$$\frac{\partial T_g}{\partial t} = \frac{k_{egax}}{\rho_g Cp_g}\frac{\partial^2 T_g}{\partial Z^2} + \frac{k_{egr}}{\rho_g Cp_g}\left(\frac{1}{r}\frac{\partial}{\partial r}\left(r\frac{\partial T_g}{\partial r}\right)\right) - \frac{h a_v}{\rho_g Cp_g \varepsilon}(T_s - T_g) - V\frac{\partial T_g}{\partial Z} \quad (4)$$

Mass balance

There is no change of composition in the packing zones so the mass balance must be written just for the reaction zone.

Gas phase

$$\frac{\partial C_g}{\partial t} = D_{eax}\frac{\partial^2 C_g}{\partial Z^2} + D_{er}\left(\frac{1}{r}\frac{\partial}{\partial r}\left(r\frac{\partial C_g}{\partial r}\right)\right) - \frac{k_g a_v}{\varepsilon_c}(c_g - C_s) - V\frac{\partial C_g}{\partial Z} \quad (5)$$

Solid phase

$$\frac{\partial C_s}{\partial t} = \frac{k_g a_v}{(1-\varepsilon)}(C_g - C_s) - \rho_s(-r_c) \quad (6)$$

The initial and boundary conditions of the energy and mass balances for the gas and solid phases in the packing and catalyst zones are:

The initial condition, $t = 0$

First cycle: Tg = finite ; Ts = finite

After the first cycle, the initial condition, for every flow reversal, is a function of position and is given by the final condition of the previous flow reversal.

The boundary conditions are:

For axial direction:

$z = 0$ (inlet)

$$V \rho_g Cp_g T_o = V \rho_g Cp_g T_g - k_{egax} \frac{\partial T_g}{\partial Z}$$

$$k_{esax} \frac{\partial T_s}{\partial Z} = h(T_s - T_g)$$

$z = L1$ and $z = L2$

$$(1-\varepsilon_p)\left[k_{esax} \frac{\partial T_s}{\partial Z}\right]_p = (1-\varepsilon_c)\left[k_{esax} \frac{\partial T_s}{\partial z}\right]_c$$

For radial direction:

$$r = 0 \quad \frac{\partial T_g}{\partial r} = 0 \; 1; \qquad \frac{\partial T_s}{\partial r} = 0$$

$r = R$

For catalyst bed

$$h_{wg}(T_g - T_w) + h_{ws}(T_s - T_w) = h_c(T_w - T_c)$$

and

$$k_{esr} \frac{\partial T_s}{\partial r} = h_{ws}(T_s - T_w)$$

$$k_{egr} \frac{\partial T_g}{\partial r} = h_{wg}(T_g - T_w)$$

For packing zones 1 and 2:

$$h_{wg}(T_g - T_w) + h_{ws}(T_s - T_w) = \frac{k_{insul}}{\Delta x_{insul}}(T_w - T_{amb})$$

For mass balance, the initial and boundary conditions are:

$t = 0$	$Cg = Cs = 0$
$z = L1$	$Cg = Co$
$z = L2$	$\partial Cg/\partial Z = 0$
$r = 0$	$\partial Cg/\partial r = 0$
$r = R$	$\partial Cg/\partial r = 0$

Non-linearity appearing in Eqs. (1) to (6) allow only numerical solution. For this study, finite difference method was used to solve the problem.

The equations used to calculate the heat removal from the reactor system are:

$$m_c Cp_c (T_{c2} - T_{c1}) = h_c A (T_w - T_b) \qquad (7)$$

and

$$T_b = \frac{T_{c2} + T_{c1}}{2} \qquad (8)$$

The outlet coolant temperature can be calculated as follows:

$$T_{c2} = \frac{h_c A T_w + T_{c1}(m_c Cp_c - h_c A/2)}{m_c Cp_c + h_c A/2} \qquad (9)$$

From these calculations, the coolant temperature for the next step for the boundary condition in the *r*-direction is calculated by assuming that the increase of coolant temperature is linear, $T_c = az + b$.

All properties for the mathematical model are obtained from the literature except for reaction rate which was obtained from the experimental data. The equation for reaction rate is:

$$(-r_c) = 0.030661\, e^{-11332.99/RT} P_{C_3H_6}^{0.73870} \qquad (10)$$

RESULTS AND DISCUSSIONS

Effect of operating variables in the stationary cycling state

The experimental results reported below show several interesting features of the reaction system such as the occurrence of a maximum temperature close to the reaction zone entrance and the occurrence of the second maximum in the first minute when the flow is reversed. These features can be understood by considering the intrinsic kinetics, the high exothermicity of the reaction and thermal inertia. Figures 2 and 3 shows the behavior expected that the maximum temperature are close to the inlet region and for first minute of operation there are two maxima. The occurrence of the maximum temperature close to the inlet region is caused by the fast exothermic reaction which rapidly consumes the

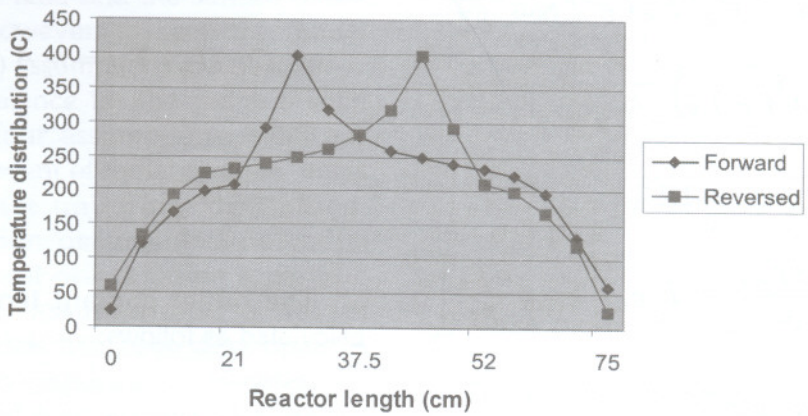

Figure 2. Temperature Distribution at the End of 15th Cycle for Forward and Reversed Flows

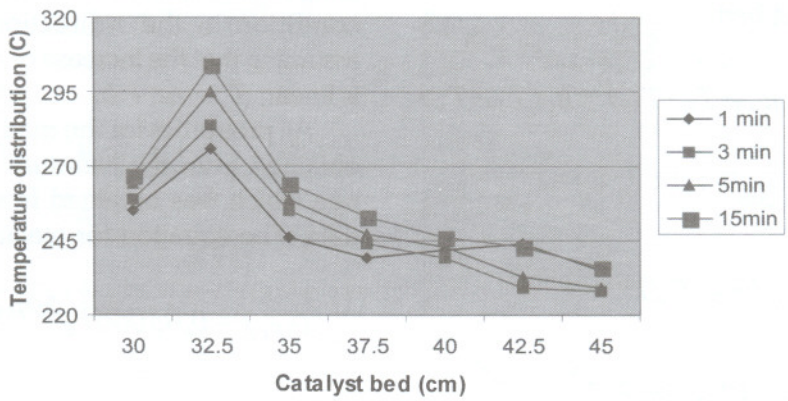

Figure 3. Temperature Distribution in the Reaction Zone at the End of 15th Cycle

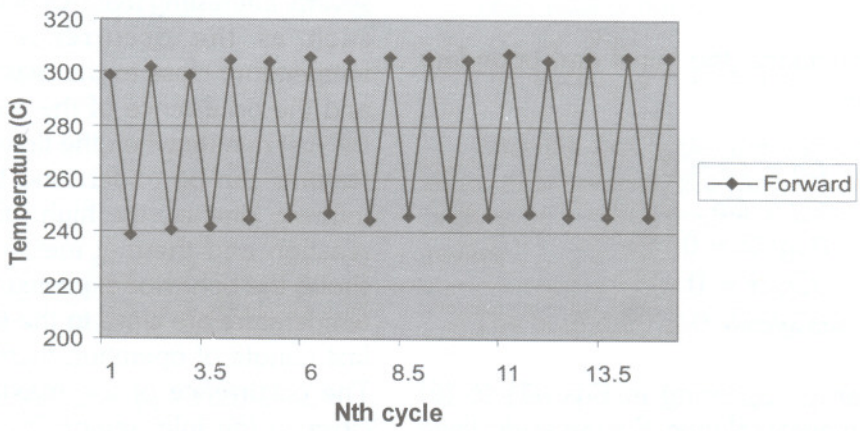

Figure 4. Temperature in the Hot Spot Location During the Cycling Process

propylene in the inlet region. The second maximum in the first minute of operation arises out of the hot spot from previous half-cycle operation. The second maximum disappears quickly since there is essentially no exothermicity in this region to maintain the heat. The cycling profiles for the temperature at the hot spot location observed at the end of each cycle, presented in Figure 4, also shows that the maximum temperature disappears when the flow is reversed and reappears in the next cycle. This happens for both forward and reversed flows.

The effect of concentration was studied by increasing the propylene concentration from 1 to 2 % while keeping the other variables at their base levels. The flow rate of air coolant used was 1,000 ml/min and the direction of the coolant was always countercurrent to the direction of the feed mixture inside the reactor. Increasing combustant concentration raises temperatures throughout the catalyst and regenerator beds; however, the shape of the temperature profiles is unchanged from those in Figure 2. As expected, the maximum measured temperature and heat removal increase with concentration as a result of the increased heat released.

Indeed, the temperature rise at the entrance of the bed as measured by the maximum temperature should be proportional to the adiabatic temperature rise. Increasing the propylene from 1 to 2 % doubles the heat released. Accompanying these changes in feed concentration, the maximum temperature increases by 95°C, while the heat removal increases by 12.7 J/min. The heat loss becomes more severe at the higher temperatures.

Further studies show that maximum temperature and heat removal are not linear in concentration. Heat loss is one reason; another is that when combustion concentration increases, the inlet temperature and the width of the hot zone region also increase. It is heat removal and heat loss that influence the ratio of the maximum measured temperature to the adiabatic temperature rise for the system.

If feed concentrations exceed a threshold, temperatures at the front of the bed rise rapidly and thermal runaway occurs. At the other extreme, the heat removal at low combustant concentration reduces bed temperatures and eventually extinguishes combustion. Although it is important to know these concentration constraints for design purposes in flow reversal, high heat losses in laboratory-scale equipment make assessment of these concentrations of doubtful value for large-scale reactors; thus, these have not been considered in this study. Nevertheless, runaway was observed in several experiments.

Because complete combustion was observed in all experiments presented in this paper, the primary effect of feed flow is on the rate of heat release in the catalyst bed. In the runs *of* this effect, flow rate was increased from 500 to 1,000 ml/min while the inlet temperature (200°C) and propylene concentration were kept constant. As flow rate doubles from 500 to 1,000 mL/min, the maximum measured temperature increases by 107.1°C for propylene oxidation. The heat removal also increases by 15.4 J/min.

The maximum temperature rise is related to the ratio of the heat released to the axial heat convection. This ratio is known as the *Damkohler number.* For this experiment, $Da = Q(-r_A)\, d_p / C_p \hat{A}_g V T = 4.903$. Q is the heat released, $(-r_A)$ is the reaction rate, d_p is the particle diameter, C_p is the gas heat capacity, $\hat{A}_g$ is the gas density, V is the volumetric flow rate, and T_g is the gas temperature.

According to Bhatia (1991) and Gupta and Bhatia (1991), in the mathematical analysis of the adiabatic flow reversal, the higher the Damkohler number, the higher is the maximum bed temperature. In addition, by doubling the flow rate, the heat release per unit catalyst volume about doubles and results in increase in maximum temperature. Therefore, the temperature profiles for doubling the flow rate should be the same as those for doubling the combustant concentration. (Bhatia 1991, Gupta and Bhatia 1991)

The hot spot location is unaffected by flow rate in the range of 500 to 1,000 mL/min, indicating that combustion is already complete in the first few centimeters of the catalyst bed. The width of the hot region increases with flow rate as a result of convective and conductive heat flows. There is a possibility that higher space velocity widens the combustion zone, which will extend also to the hot region.

The ratio of the maximum measured temperature rise to the adiabatic temperature rise, calculated as $(T_{max} - T_{in}) / T_{ad}$, and the percentage

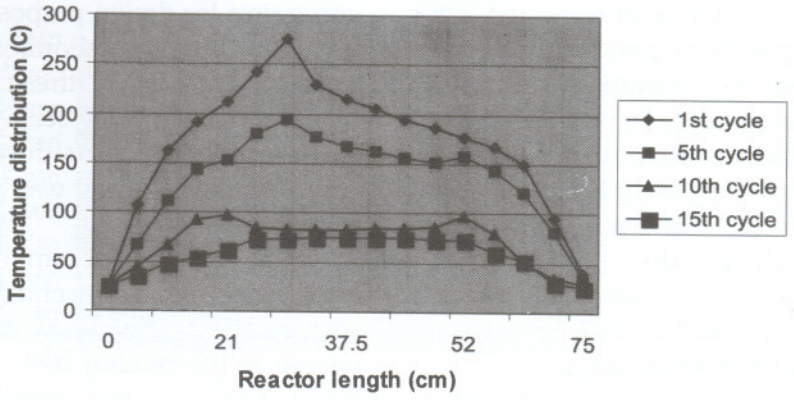

Figure 5. Temperature Distribution after 15 min

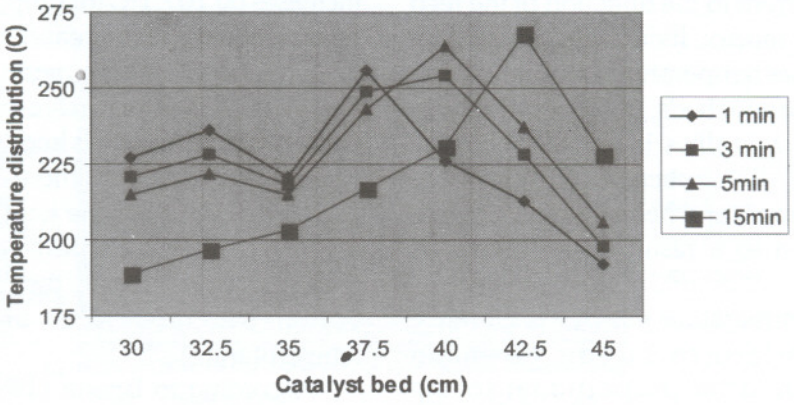

Figure 6. Temperature Distribution in the Reaction Zone at the End of 1st Cycle

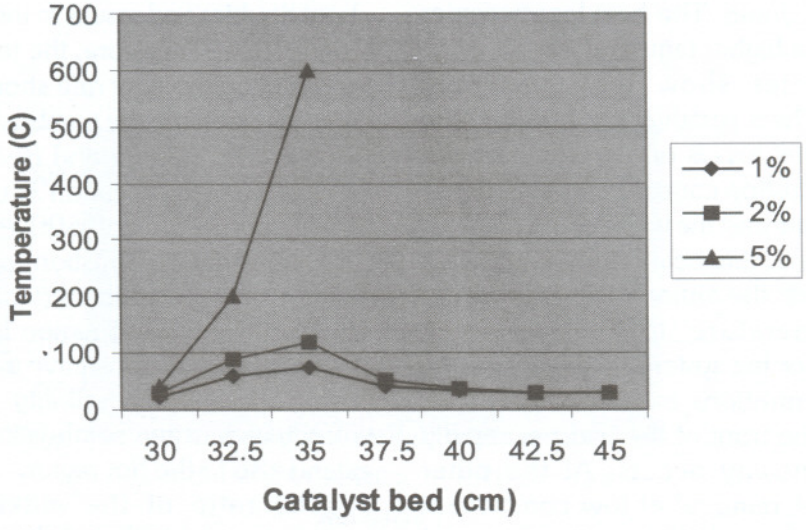

Figure 7. Effect of Propylene Concentration on the Temperature Profile

of the heat removal by the coolant from the total heat released by the reaction have also been studied as functions of the propylene concentration in the feed. The result shows that the higher the concentration of propylene, the lower the ratio of maximum temperature rise to the adiabatic value and the lower the percentage of heat release that is removed via coolant.

These phenomena are caused by the heat loss in the radial direction from the concentric heat exchanger as a result of insufficient insulation as well as heat storage in the insulation. Higher concentrations produce higher maximum temperatures which create larger temperature differences between the system and the surroundings, thereby causing greater heat losses. This situation has also been observed by Matros (1989) in an adiabatic flow reversal reactor for methane combustion. This experiment showed that by increasing the concentration of methane from 0.48 to 0.66 %, the heat recovery decreased from 51 to 34%. The heat loss for this experiment was estimated as follows:

$$Q_{release} = Q_{exhaust} + Q_{coolant} + Q_{heat\ loss} \qquad (11)$$

where

$$Q_{release} = V_g C_o (-\Delta H) \Delta t_{cycle}$$

$$Q_{exhaust} = V_g \rho_g C_p (T_{exhaust} - T_o) \Delta t_{cycle}$$

Q is the quantity over the cycle, T_o is the inlet temperature, V_g is the volumetric flow rate in ml/min, ρ_g is the gas density in g/ml, C_o is the concentration of the gas in mol/ml, C_p is the gas capacity in J/g °C, and $(-\Delta H)$ is the heat of reaction in J/mol. Using Eq. (11), the heat loss for 1% propylene is 284 J/min, or 65% of heat released from the reaction.

The steady state experiments by Dhalewadikar (1984) for catalytic combustion of ethylene using supported platinum catalyst in a nonadiabatic fixed bed reactor also support the findings of this study. He shows that when the combustant concentration in the feed mixture is increased, the maximum temperature also increased. However, the ratio of the maximum temperature rise to the adiabatic temperature rise in his study also suggest a large heat loss in both the radial and axial directions. This researcher also found that the higher the combustant concentration, the greater is the heat loss from the system. By increasing the concentration of ethylene from 0.5 to 1 %, the ratio decreases from 18.09 to 15.11 %.

Provided the cycle is not too long as to permit the cooling front in the upstream regenerator to penetrate the catalyst bed and thereby blow out combustion, the cycle period will have only a small effect on the temperature profile in the catalyst bed and on the heat removal through the coolant. All measurements were made in the 15th cycle just before a flow direction change occurred. These results show that cycle period is not an important operating variable.

Results of dynamic cycling state

Excessive cooling

To examine the phenomena in the flame out caused by excessive cooling, the researcher used the results of propylene oxidation with water coolant. The main objective of the experiments using water as a coolant was to generate steam and thus to have a more uniform coolant temperature as well as to increase the rate of heat transfer between the coolant and the reactor wall.

The experimental results show that no single run was carried out for 15 cycles; the longest achieved was 9 cycles. The cause was the quenching of the reactor by the coolant. Thus, the oxidation was eventually extinguished by this cooling load after several cycles. Excessive cooling is shown by the 15 min profile in Figures 5 and 6 which drops below the initial temperature at the end of the catalyst bed. When the direction of flow is reversed, the inlet temperature will be too low for ignition. Ignition occurs in the center. Then the figure shows that there is a backward movement of the thermal waves. This occurs because the region at the end of the reaction zone is still cold when the flow is reversed (the temperature is below the inlet temperature needed to start the reaction).

This cold region cannot be used to activate the reaction fully when the flow is reversed. Therefore, after flow reversal the reactant mixture must travel to the middle of the reactor in order

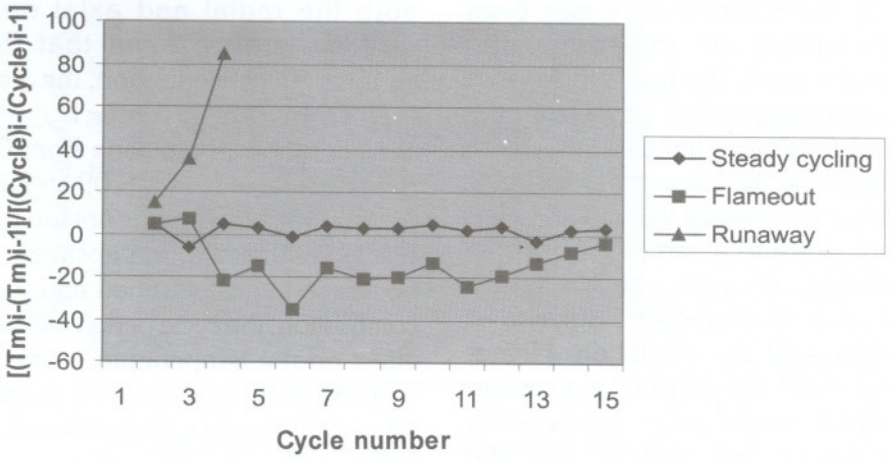

Figure 8. RTC, for Runaway, Flame Out, and Steady Cycling

to be heated to ignition. Once ignited, its exothermicity moves it closer to the inlet of the reactor. The net result created a backward movement of the hot region in the reactor. Further experiments show that increasing the number of cycles totally extinguishes the reaction.

Runaway

Runaway was found when the feed concentration was high and exceeded 5%. When runaway occurs, the maximum measured temperature and heat removal increase sharply and can go up to more than 1,000 J/min.

Experiment on the temperature distribution within the cycle demonstrated that (a) the maximum measured temperature occurring at the region close to the feed inlet and (b) there are secondary local maximum temperatures at the end of the catalyst bed for first-minute operation. The experiment also showed that the rate of increase of the maximum measured temperature from first minute to the end of half cycle becomes greater as the number of cycle increases. However, investigation of the temperature changes in the packing zones; show that the temperatures in both packing zones are not greatly affected by the temperature rise in the catalyst zone.

Table 2. Slope of Experiments for Runaway, Flame Out, and Steady Cycling State

Cycle	Slope		
	Steady Cycling	Flame Out	Runaway
2nd Cycle	21.2	17.4	40.1
3rd Cycle	21.7	9.5	116.9

Identification of flame out and runaway

In the nonadiabatic flow reversal experiments, runaway and flame out can occur after several cycles. The slowness of these two process means that remedial action can be taken if flame out and runaway behavior can be identified. This section deals with identification. Three approaches seem possible based on the results presented in the earlier section:

1. Calculation of the rate of increase or decrease of the maximum measured temperature at the end of half cycle over cycle number using the following equation:

$$RTC = \frac{\Delta T_{\max}}{\Delta cycle} = \frac{(T_{\max})_i - (T_{\max})_{i-1}}{(cycle)_i - (cycle)_{i-1}} \qquad (12)$$

2. For convenience, for calculation of the rate of increase or decrease of the maximum measured temperature within a cycle, a five-minute time increment was used:

$$RTT = \frac{\Delta T_{\max}}{\Delta t} = \frac{(T_{\max})_i - (T_{\max})_{i-1}}{t_i - t_{i-1}} \qquad (13)$$

3. By calculating the slope of temperature distribution in the bed front as follows:

$$Slope = \frac{T_{32.5} - T_{30}}{32.5 - 30}$$

For the first method, when the runaway occurs, RTC is positive and much greater than zero while RTC is negative and less than zero when the system is extinguished. Figure 8 shows the RTC for runaway, flame out, and results of steady cycling state. It can be seen from the figure that for stable operation the calculated RTC is close to zero after 2nd cycle. In addition, the higher the cycle number, the higher is the RTC for the runaway. The RTC for flame out does not change significantly with increasing cycle numbers.

The identification of unstable behavior using the second method can only be applied to the runaway since there is moving wave within cycling for flame out behavior. When runaway occurs, RTT increases with increasing time. Reversely, however, for stable operation, the RTT should go down to zero with increasing time.

The third method, the identification of runaway and flame out by calculating the slope of the temperature at the inlet of the catalyst bed is shown in Table 2. The temperatures for the test were taken at 30 and 32.5 cm positions, respectively, with the catalyst bed at 30 cm. The table compares the slopes of the temperature profiles between the 2nd and 3rd cycles for flame out, runaway, and steady cycling state.

On the one hand, when runaway occurs, the temperature at both points increase and so does the slope. On the other hand, the temperature at both points and the slope decrease when the system dies out. The table shows that there are only small changes in the slope for stable operation, although the temperature at both points increase.

It appears that all three approaches are capable of indicating unstable operation. The slope method seems easiest to use as it can be applied between cycles, such as in Table 2, or used within a cycle. If a feed condition or coolant change occurs at a point within a cycle, this can be detected in the change in slope.

Results of mathematical modeling

Figure 9 shows an example of predicted axial temperature profiles along the reactor system and the experimental data. The figure shows differences in the temperature profiles for the experiment and the simulation, possibly as a result of factors such as neglecting the unsteady state process on the catalyst surface and estimating rather than measuring parameters.

The reaction rate expressions were obtained experimentally (Purwono 1997); however, several parameters (k_{esax}, k_{egax}, k_{esr}, k_{egr}, h_{wg}, and h_{ws}) had to be estimated from published composite values that included both solid and gas phases. In addition, uncertainties occured in the experimental data themselves, since a sizable heat loss (40–60%) was noted in the overall energy balance. This heat loss though was not represented

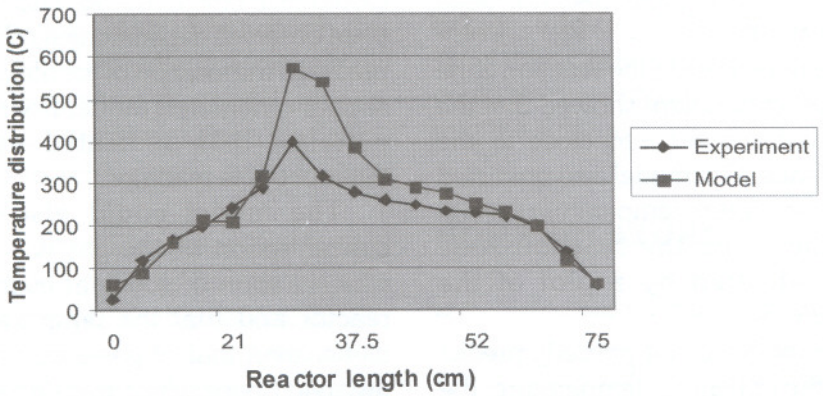

Figure 9. Example of the Predicted Axial Temperature Profiles Along the Reactor System

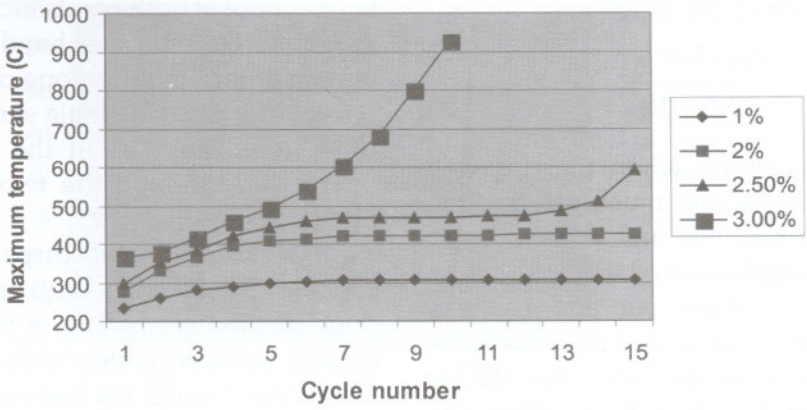

Figure 10. Effect of Propylene Concentration on the Maximum Temperature

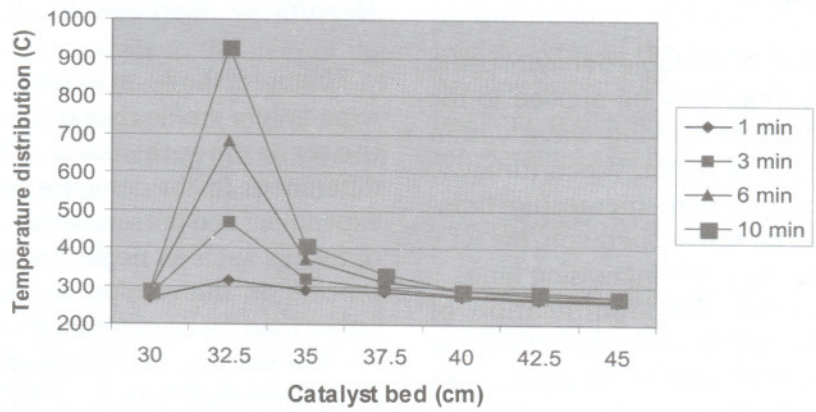

Figure 11. Temperature Distribution in the Catalyst Bed During Runaway

well by the model. By neglecting the discrepancy in the magnitudes of the maximum temperatures the shape of the profile predicted in the simulation would agree with the experimental observations. As can be seen in the figures, the model predicts the occurrence of a maximum temperature though this temperature is somewhat overpredicted because heat loss had not been allowed for in the simulation.

The temperature profiles in the reaction zone for both model and experiment showed that the maximum temperatures occured close to the reaction zone entrance. The model also predicted the location of the maximum temperature several centimeters farther from the reaction zone entrance than indicated by a plot of the thermocouple readings.

Although the model did not properly predict the magnitude of the maximum temperature, the model could also predict the occurrence of the second maximum temperature in the first minute after the flow had been reversed.

There was a time during which two temperature peaks occured. After flow had been reversed, thermal peaks would start to grow in the cool end of the bed as a result of combustion. The "old" thermal peak, however, now downstream, would take time to decay. This phenomenon had been observed experimentally also. The model also predicted the location of the maximum temperature several centimeters farther from the reaction zone entrance than indicated by a plot of the thermocouple readings.

The model could also show that the concentration of the gas was higher than the concentration of solids at every position of the reactor and that the temperature of solids is higher than that of gases due to the reaction in the solid phase which transferred heat to the gas phase. Once the maximum temperature is

achieved, the gas temperature becomes higher than the solid temperature because the catalyst bed is being heated by the gas. The difference between the temperatures of fluids and solids was seen to be very minimal, despite the strongly exothermic nature of the reaction. This had been expected because gas–solid heat transfer had been rapid.

For the experiment, there was no direct measurement of the axial concentration profiles. Thus, only the total conversions could be compared for the model and the experiment. Nevertheless, the concentration profiles had been helpful in explaining the behavior of the axial temperature distribution.

In the experiment, the maximum temperature was explained by a large reaction exothermicity that elevated the catalyst temperature and increased the reaction rate, resulting in the rapid consumption of large amounts of reactants. The concentrations of propylene and oxygen decreased rapidly in the region close to the inlet of the reaction zone, while the temperature increased rapidly in the same region.

Sensitivity analysis of variables

It is well known in reaction engineering that for highly exothermic reactions, the reaction rate is a strong function of reactant concentration. Therefore, changes in feed concentration have significant effects on the reaction rate and on other related processes. In addition, for such reactions, increasing the concentration increases both reaction rate and surface temperature.

This section is devoted to the sensitivity of the system due to changes of concentration.

The results of the study of variable sensitivity are shown in Figures 10 and 11. Although the model does not properly predict the magnitude of the maximum temperature, the model can also predict the *occurrence* of runaway. From the figure, it can be seen that small changes in concentrations can lead to runaway.

Figure 10 also shows another interesting phenomenon: that runaway is not necessarily instantaneous and can occur after several cycles. Further simulation on the temperature distributions within a cycle for runaway situation show that increasing the maximum measured temperature from the first minute to the end of half cycle (after 15 min) becomes faster when the number of cycle increases, which has also been observed in the experiment.

Further studies in the variation of coolant flow rate shows that runaway can be prevented by using higher coolant flow rates. This is expected since the more rapid removal of heat by the coolant decreases the maximum temperature, preventing runaway. Thus, one of the main objectives of this study, to demonstrate that an integral heat exchanger reactor can prevent runaway, has been achieved.

CONCLUSIONS

A laboratory-scale nonadiabatic-flow reversal reactor with integral heat exchanger [?], using Pt / zeolite catalyst was successfully operated on a dilute propylene stream of 1–2% propylene. This integral heat exchange functioned well with 15 to 25 % of the heat of reaction removed from the system. The maximum bed temperature was experimentally found sensitive to changes in both feed flow rate and reactant concentration, but not to the length of a cycle.

The detailed models predicted the behavior of nonadiabatic flow reversal but inadequate allowance for heat loss made the model overpredict the effects of the operational variables on the temperature profiles and heat removal. The simulation results for the variation of concentrations showed the experimentally observed behavior. When concentration increased, maximum temperature also increased.

Further simulations showed that runaway could occur when concentration was high and that it is not necessarily instantaneous and could occur suddenly after several cycles. These simulations, however, also showed that runaway could be prevented by flowing sufficient coolant into the system.

NOMENCLATURE

a_v	area per unit volume, cm^{-1}
Cp_g	gas heat capacity, *cal/g °C*
Cp_s	solid heat capacity, *cal/g °C*

h	gas–solid heat transfer coefficient, cal/ cm^2 °C s
k_{egax}	gas axial effective conductivity, cal/ cm °C s
k_{egr}	gas radial effective conductivity, cal/ cm °C s
k_{esax}	solid axial effective conductivity, cal/ cm °C s
k_{esr}	solid axial effective conductivity, cal/ cm °C s
r	bed radius, *cm*
r_c	reaction rate, *mol/gcat s*
T_g	gas temperature, °C
T_s	solid temperature, °C
V	mean velocity, *cm/s*
Z	bed length, *cm*

Greek letters

ΔH	heat of reaction, *cal/mol*
ε	bed void fraction
ρ_g	gas density, g/cm^3
ρ_s	particle density, g/cm^3

ACKNOWLEDGMENTS

The author is grateful for funding from Indonesian Research Council (DRN) through the RUT project.

REFERENCES

Bhatia, S. K. (1991)., *Chem. Eng. Sci., 46,* 1, 361.

Blanks, R. F., Wittrig, T. S., and Peterson, D. A. (1990). *Chem. Eng. Sci., 45,* 8, 2407.

Boreskov, G. K., and Matros, Y. S. (1983). *Catal. Rev. Sci. Eng., 25,* 551.

Boreskov, G. K., Matros, Y. S., Kiselev, O. V., and Buminovich, G. A. (1977). *Dokl. Akad. Nauk SSSR, 237,* 1, 160.

Boreskov, G. K., Matros, Y. S., and Ivanov, A. G. (1986). "Carrying out of a heterogeneous catalytic process under non-steady-state condition," *Dokl. Akad. Nauk SSSR, 288, 2,* 429, 1986.

Eigenberger, G., and Nieken, U. (1988). *Chem. Eng. Sci., 43,* 8, 2109.

Froment, G. F. (1990). In *Unsteady-state processes in catalysis,* Matros, Y. S., ed., VSP, Utrecht.

Gawdzik, A., and Rakowski, L. (1988). *Chem. Eng. Sci., 43,* 11, 3023.

Gawdzik, A. and Rakowski, L. (1989). *Computers Chem. Eng., 13,* 10, 1165.

Gupta, V. K., and Bhatia, S. K. (1991). *Computers Chem. Eng., 15,* 4, 229.

Matros, Yu. Sh. (1985). *Unsteady processes in catalytic reactor,* Elsevier, New York.

Matros, Yu. Sh. (1989). *Catalytic processes under unsteady-state conditions,* Elsevier, New York.

Matros, Yu. Sh. (1990). *Unsteady-state processes in catalysis,* VSP, Utrecht.

Purwono, S. (2002). "CO oxidation over metal oxide catalyst supported by Indonesian Natural Zeolite," *ASEAN Journal of Chemical Engineering, 2,* 1, 38.

Purwono, S., Hudgins, R. R., and Silveston, P. L. (1992). "Unsteady-state catalytic combustion," *Proc. 12th Can. Sympos. Catal.,* Banff, Alberta, Canada.

Purwono, S., Budman, H., Hudgins, R. R., Silveston, P. L., and Matros, Y. S. (1994). "Runaway in packed bed reactors operating with periodic flow reversal," *Chem. Eng. Sci, 49,* 24 B, 5473.

Purwono, S., Murachman, B., Triono, Hardjono, Budhijanto, and Witono, H. (1997). "Development of platinum and palladium catalyst for oxidizing waste gases," *Forum Teknik, 21,* 2, 229.

Rehacek, J., Kubicek, M., and Marek, M. (1992). *Chem. Eng. Sci., 47,* 9, 2897.